Applied Catalysis B: Environmental 206 (2017) 9–15

Contents lists available at ScienceDirect

Applied Catalysis B: Environmental

journal homepage: www.elsevier.com/locate/apcatb

MIL-68(Fe) as an efficient visible-light-driven photocatalyst for the treatment of a simulated waste-water contain Cr(VI) and Malachite Green

Fenfen Jing[a], Ruowen Liang[a], Jinhua Xiong[a], Rui Chen[a], Shiying Zhang[b], Yanhua Li[b], Ling Wu[a,*]

[a] State key laboratory of photocatalysis on energy and environment, Fuzhou University, Fuzhou 350002, PR China
[b] Hunan Province Key Laboratory of Applied Environmental Photocatalysis, Changsha University, Changsha 410022, PR China

ARTICLE INFO

Article history:
Received 21 October 2016
Received in revised form
26 December 2016
Accepted 30 December 2016
Available online 4 January 2017

Keywords:
MIL-68(Fe)
Photocatalysis
Cr(VI)
Visible light

ABSTRACT

A highly effective Iron Metal-Framework photocatalyst (MIL-68(Fe)) has been successfully prepared via a facile solvothermal method under acidic condition. The UV–vis diffuse reflectance spectrum reveals that the absorption edge of MIL-68(Fe) is 440 nm. The flat-band potential of MIL-68(Fe) is −0.6 V *vs.* NHE at pH = 6.8, which is more negative than the redox potential of Cr(VI)/Cr(III) (+0.51 V, pH = 6.8). Consequently, it is thermodynamically permissible for the transformation of photogenerated electrons to the Cr(VI) to produce Cr(III). Moreover, MIL-68(Fe) could perform as an efficient photocatalyst towards the reduction of Cr(VI) aqueous with a wide pH range. After 5 min of visible light illumination (λ > 420 nm), almost 100% Cr(VI) can convert to Cr(III) with $(NH_4)_2C_2O_4$ as a scavenger (pH = 3), which is also higher than that of N-doped TiO_2 (50%) and ZnO (7.6%) under identical conditions. Furthermore, MIL-68(Fe) is proved to perform as a highly efficient photocatalyst for remove of different aqueous contaminant with malachite green (MG) as a scavenger. Finally, a possible reaction mechanism has also been investigated in detail.

1. Introduction

Hexavalent chromium species (Cr(VI)) are highly toxic substances have been regarded as carcinogens, mutagens and teratogens in biological systems. They mainly arise from industrial waste-water, for instance, tanning, metallurgy, plating and metal finishing [1]. The researches have shown that excessive concentrations of Cr(VI) will have lethal effects to aquatic life and the levels of chromium in water should be reduced to 0.1 ppm [2]. Consequently, the removing of Cr(VI) from wastewater is an urgent need. To date, many techniques have been adopted for Cr(VI) removing, such as reduction, precipitation, ion exchange, reverse osmosis and photocatalytic reduction [1,3,4]. Because of its clean and environmentally friendly and relatively effective, photocatalytic reduction technology has attracted great interest. It is well-known that TiO_2-based or ZnO-based photocatalysts could exhibit considerable activity for removing Cr(VI) [5,6]. Unfortunately, these materials show a low utilization rate of solar energy in the photocatalytic reaction. Therefore, it is necessary to explore efficient novel visible-light-driven photocatalysts.

Metal-organic frameworks (MOFs) have been aroused great attention in the past decade, because of their spatial structure, large surface area and pore volume [7,8]. Up to now, MOFs have been successfully applied in gas storage, adsorption, separation, catalysis and drug delivery [9–13]. Since the first report on photocatalytic activity in MOF-5, more and more MOFs such as Ni-MOF [14], MIL-101(Cr) [15], NH_2-MIL-68(In) [11] and NH_2-UiO-66(Zr) [16] can behave as pseodo-semiconductors. Among MOFs materials, Fe based Metal-organic frameworks material (Fe-MOFs) have becoming a promising photocatalysts owing to their high chemical stability, non-toxic, low cost and photosensitivity [17]. In our previous works, MIL-53(Fe) and MIL-100(Fe) were found to show good photocatalytic performances under visible light [17–19]. As one of Fe based metal-organic framework, Fe-benzenedicarboxylate (MIL-68(Fe)) was first reported by Gérard Férey group, which consists of chains of corner-sharing $Fe(OH)_2O_4$ octahedral connected through a BDC(terephthalic acid) linker [20]. Compared with other Fe-MOFs, the reports on MIL-68(Fe) for photocatalytic applications are rather scarce [21,22]. Especially, utilization of MIL-68(Fe) for photocatalytic reduction under visible light has remained unavailable so far.

* Corresponding author at: State Key Laboratory of Photocatalysis on Energy and Environment, Fuzhou University, Fuzhou 350002, PR China.
E-mail addresses: wuling@fzu.edu.cn, 2307422493@qq.com (L. Wu).

http://dx.doi.org/10.1016/j.apcatb.2016.12.070
0926-3373/

Herein, we have reported photocatalytic performance of MIL-68(Fe) for the reduction of Cr(VI) to Cr(III) under visible light irradiation. Meanwhile, the factors that affect the Cr(VI) reduction, such as the pH value of the reaction solution has also been investigated in detail. Fortunately, MIL-68(Fe) could also perform as a difunctional photocatalyst for the treatment of different types of water contaminants (the mixed of dyes and Cr(VI)), simultaneously. Finally, a possible reaction mechanism of photocatalytic reduction of Cr(VI) and degradation of dye (MG) solutions through MIL-68(Fe) have also been investigated in detail.

2. Experimental

2.1. Materials and reagents

Iron(III) chloride hexahydrate ($FeCl_3{\cdot}6H_2O$) was supplied by Aladdin Reagent Co., Ltd. 1,4-benzenedicarboxylic acid (H_2BDC) was obtained from Alfa Aesar China Co., Ltd., potassium dichromate ($K_2Cr_2O_7$), sulfuric acid (H_2SO_4), hydrochloric acid (HCl), N,N-Dimethylformamide (DMF), hydrofluoric acid (HF, 49%), Malachite Green (MG), ZnO and ammonium oxalate ($(NH_4)_2C_2O_4$) were obtained from Sinopharm Chemical Reagent Co., Ltd. (Shanghai, China). All materials were used as received without further purification. N-TiO_2 was prepared by laboratory.

2.2. Synthesis of MIL-68(Fe) samples

MIL-68(Fe) was obtained according to the strategy that reported in previous [20,21]. A mount of $FeCl_3{\cdot}6H_2O$ and H_2BDC (molar ratio = 1:2) were mixed with 12 mL DMF in a Teflon-lined autoclave, then 120 μL HF (5 mmol) and 120 μL HCl (1 mmol) were added, followed stirring for another 30 min to blend completely. After that, the Teflon-lined was heated at 100 °C for 120 h. The products were left cool at room temperature, collected by centrifugation and washed with deionized water and acetone several times to eliminate the DMF molecules in the pores. Finally, the recovered solid was dried at 100 °C vacuum oven for 24 h.

2.3. Characterizations

The X-ray diffraction (XRD) patterns of the samples were carried on a Bruker D8 Advance X-ray diffrractometer operated at 40 kV and 40 mA with Ni-filtered Cu Ka irradiation. The data were recorded in the 2θ ranging from 3° to 50° with a step width of 0.05°. UV–vis diffuse reflectance spectra (UV–vis DRS) were obtained by a Cary 500 UV–vis–NIR spectrophotometer in which $BaSO_4$ powder was used as the internal standard to obtain the optical properties of the samples over a wavelength range of 200–800 nm. X-ray photoelectron spectroscopy (XPS) measurements were conducted on a PHI Quantum 2000 XPS system equipped with a monochromatic Al Kα X-ray source to obtain the surface elemental composition of the sample. The Fourier transformed infrared spectra (FTIR) was carried out on a Nicolet Nexus 670 Fourier transform infrared spectrometer. The Mott–Schottky analysis was performed at a Zenuium electrochemical workstation. The electrochemical measurements were performed in a conventional three electrode cell, Ag/AgCl electrode was used as the reference electrode and a Pt plate was used as the counter electrode. The working electrode was prepared on fluorine-doped tin oxide (FTO) glass, which was previously cleaned by ethanol and deionized water. The slurry was obtained from 5 mg photocatalyst which ultrasonicated in 0.5 mL of *N*, *N*-dimethylformamide, then dip-coated on the surface of the FTO glass, whose side part was previously protected using Scotch tape. After dried overnight under nature conditions, a copper wire was connected to the side part of the FTO glass using conductive tape. The working electrodes were immersed in a 0.2 M Na_2SO_4 (pH = 6.8) aqueous solution without any additive for 30 s before measurement.

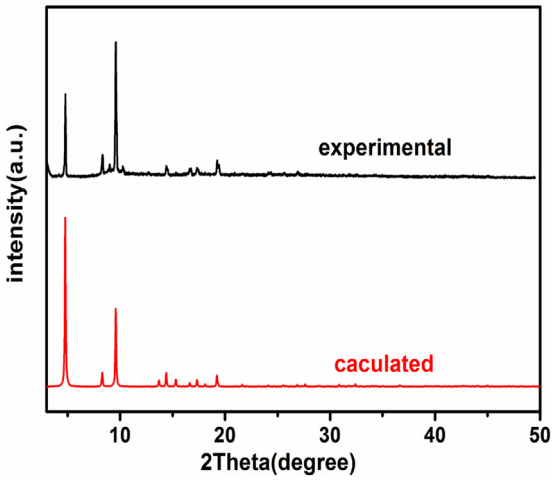

Fig. 1. XRD patterns of the as-prepared and calculated MIL-68(Fe).

2.4. Evaluation of photocatalytic activity

The photocatalytic activity of the prepared samples was evaluated by reduction of aqueous Cr(VI) under visible irradiation. In a typical reaction, 10 mg photocatalysts and 5 mg $(NH_4)_2C_2O_4$ were added into 40 mL of 20 ppm Cr(VI) solution in a 100 mL quartz vial. The pH values of solutions were adjusted with H_2SO_4 (2 mol L^{-1}). Before illumination reaction started, the suspension was stirred in the dark for 40 min to establish the adsorption–desorption equilibrium between the samples and the reactant. For this experiment, an ozone-free 300 W Xe lamp (PLS-SXE 300C, Beijing Perfect light Co. Ltd.) with 420 nm cut-off filter was used as the light source (420 nm < λ < 760 nm) to trigger the photocatalytic reaction. During the illumination reaction process, about 3 mL reaction solution was collected at a certain time interval then centrifuged at 7000 rpm for 5 min to remove the catalyst completely. The reduction amount of Cr(VI) was analyzed on a Varian ultraviolet-visible-light (UV–vis) spectrophotometer (Cary–50, Varian Co.) and determined colorimetrically at 540 nm using the diphenyl-carbazide method [23]. The reduction ratio of Cr(VI) is calculated using the following expression:

$$\text{ReductionratioofCr(VI)} = (C_0 - C_t)/C_0 \times 100\%$$

Where C_0 and C_t are the absorbance intensities of illuminated for 0 and t min, respectively.

3. Results and discussion

3.1. Characterizations

XRD patterns of as-prepared samples and calculated MIL-68(Fe) are shown in Fig. 1. It is obvious that the diffraction peaks of MIL-68(Fe) match well with the calculated ones, indicating that the obtained samples are pure phase. In addition, the Fourier transformed infrared spectroscopy (FTIR) has been performed to analyze the molecular structure of MIL-68(Fe). As displayed in Fig. 2, the peak at 550 cm^{-1} can be ascribed to the stretching vibration of Fe–O, indicating the formation of a metal-oxo bond between the carboxylic group of terephthalic acid and the Fe(III) [24]. The peak at 748 cm^{-1} corresponds to C–H bonding vibrations of the benzene rings [25,26]. Moreover, the adsorption band of the carboxyl groups of the ligand coordinated to the metal centers (C=O, C–O) are

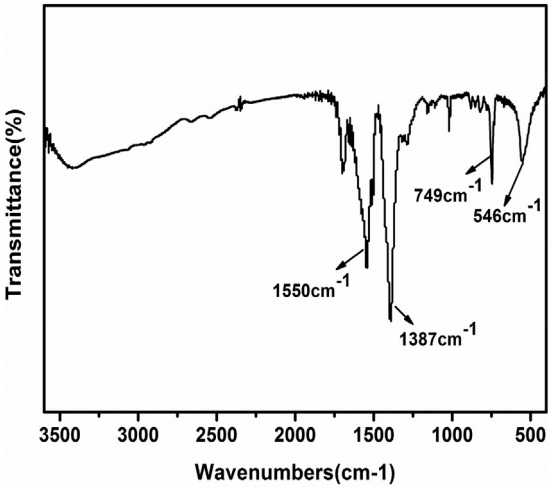

Fig. 2. FTIR spectrum spectra of MIL-68 (Fe).

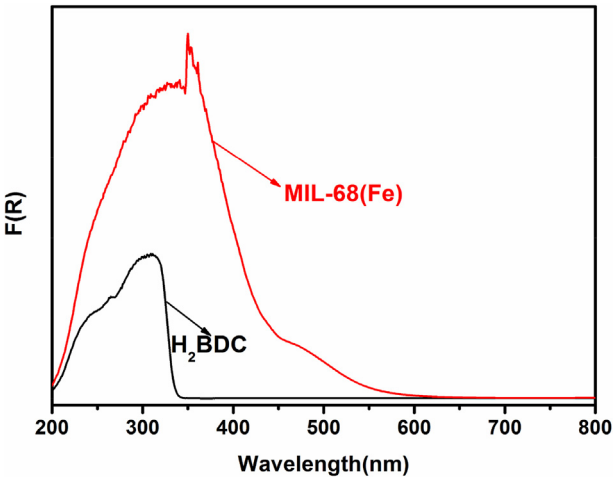

Fig. 4. UV–vis DRS spectrum of H_2BDC and MIL-68 (Fe).

located at 1550 cm^{-1} and 1387 cm^{-1} [25]. Hence, the FTIR results further identify the MIL-68(Fe) has been prepared successfully.

The X-ray photoelectron spectra (XPS) of the as-synthesized MIL-68(Fe) have been performed. As shown in Fig. 3A, C, O and Fe presence in the MIL-68(Fe). Fig. 3B exhibits the high-resolution XPS spectrum of the C 1s, which can be deconvoluted into two peaks, corresponding to the carbon components on the benzoic at binding energy of 284.6 eV and the carboxylate (O—C═O) groups of the terephthalate linkers at binding energy of 288.58 eV [27]. The high-resolution XPS spectrum of the O 1s (show in Fig. 3C) could be fitted into two peaks at binding energy of 529.90 and 531.78 eV, which correspond to the oxygen components on the Fe—O bonds and the terephthalate linkers (C═O) of MIL-68(Fe) [28,29]. As shown in Fig. 3D, the peaks of 2p region XPS spectrum for Fe are fixed at 712.11 eV (Fe $2p_{3/2}$) and 725.74 eV (Fe $2p_{1/2}$). Moreover, the satellite peaks obtained at 718.45 eV and 732.58 eV are clearly distinguishable, which are the satellites peak of Fe(III) $2p_{3/2}$ and Fe(III) $2p_{1/2}$, respectively [30,31].

Fig. 4 shows the UV–vis diffuse reflectance spectrum (UV–vis DRS) of H_2BDC and MIL-68(Fe). H_2BDC only has response in the wavelength range of 200–340 nm. The absorption band of MIL-68(Fe) appears at ultraviolet region that attributes to charge transfer of the framework oxygen to isolated transition metal ions (LMCT), while the absorption band extending into the visible light region can be ascribed to the existence of $Fe(OH)_2O_4$ in MIL-68(Fe). Previous reports have illustrated that the existence of extensive Fe-O clusters in the structure can give rises to a band in the visible region [32,33]. The band in the low energy region between 452–600 nm is attributed to the $d \rightarrow d^*$ transition of Fe^{3+} ions [34]. Obviously, the obtained sample exhibits an absorption

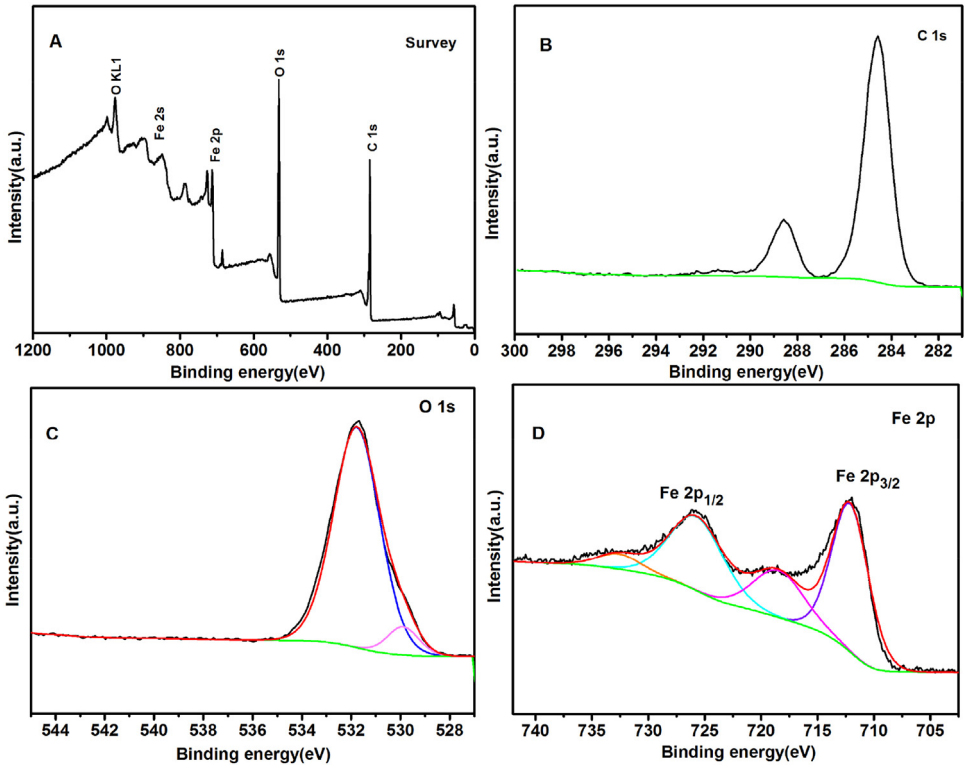

Fig. 3. XPS spectra of surface elements of the MIL-68 (Fe): (A) Survey spectrum, (B) C element, (C) O element, (D) Fe element of MIL-68 (Fe).

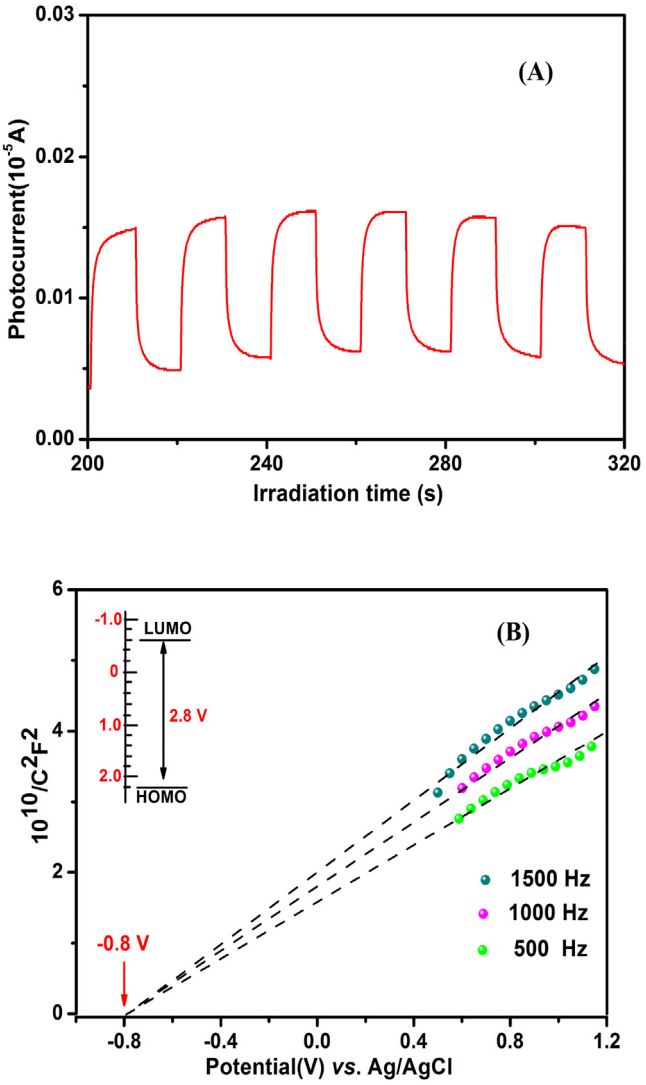

Fig. 5. Typical Mott–Schottky plots (A) and transient photocurrent spectra (B) of MIL-68 (Fe) in 0.2 M Na_2SO_4 aqueous solution (pH = 6.8).

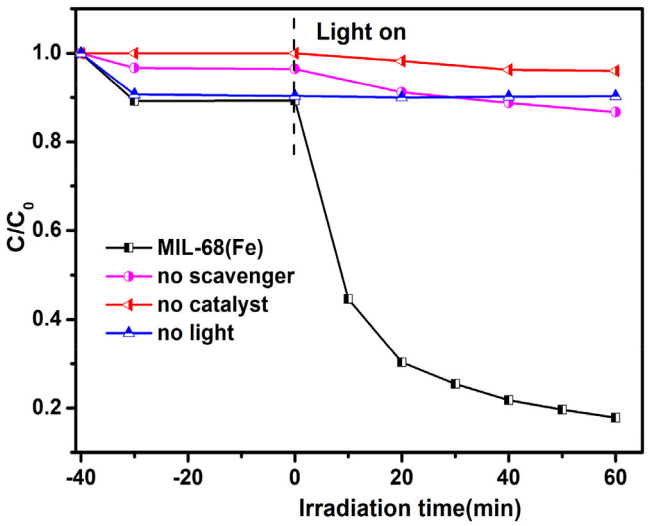

Fig. 6. Photocatalytic reduction of aqueous Cr(VI) under different conditions. Reaction conditions: 10 mg photocatalyst, 40 mL of 20 ppm Cr(VI), 5 mg $(NH_4)_2C_2O_4$.

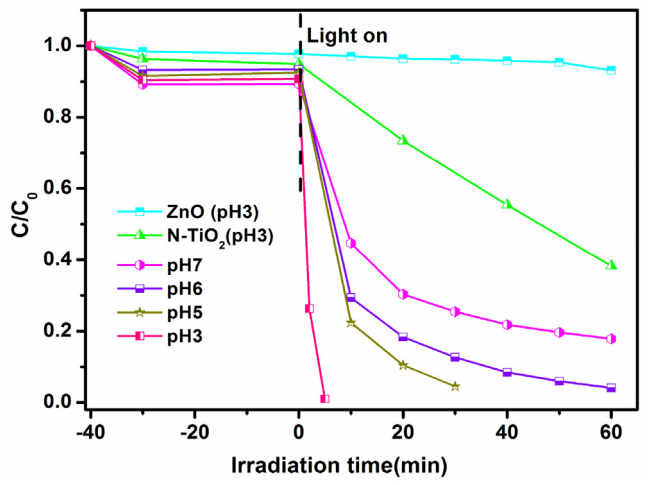

Fig. 7. Photocatalytic activities of MIL-68(Fe), ZnO and N-TiO_2 for the reduction of aqueous Cr (VI) at different pH values.

edge at 440 nm, which corresponds to 2.8 eV of band gap based on the empirical formula $E_g = 1240/\lambda$, implying MIL-68(Fe) could be shown a visible light response.

The transient photocurrent spectra of MIL-68(Fe) under intermittent visible light illumination ($\lambda > 420$ nm) has been performed. Fig. 5A shows an apparent photocurrent response of MIL-68(Fe) electrodes that over on-off cycles of intermittent visible light irradiation. This proves that MIL-68(Fe) is able to stimulate to produce electron–hole pairs under visible irradiation. The Mott–Schottky measurement has been used to comprehend the intrinsic electronic properties of MIL-68(Fe). As shown in Fig. 5B, the positive slope of the obtained C^{-2}-E plot illustrates that the as-prepared samples shows the typical behavior of an n-type semiconductor [35]. The flat-band potential of MIL-68(Fe) is around ca. −0.8 V *vs.* Ag/AgCl at pH 6.8, equivalent to −0.6 V *vs.* NHE at pH 6.8, which is more negative than that of Cr(VI)/Cr(III) (+0.51 V, pH 6.8) [36]. Consequently, it is thermodynamically permissible for the transformation of photogenerated electrons to the Cr(VI) to produce Cr(III).

3.2. Reduction of Cr (VI)

The photocatalytic performance of the as-prepared MIL-68(Fe) is initially examined by reduction of Cr(VI) in water under visible light illumination. As shown in Fig. 6, it can be seen that the reduction of Cr(VI) hardly occurs in absence of light, photocatalyst and hole scavenger (the reduction ratio of Cr(VI) is 0% and 4.0% and 8.0%, respectively). In contrast, it proceeds smoothly when the solution in presence of photocatalyst and hole scavenger under visible light illumination. The reduction ratio of Cr(VI) is 76.0% after visible light illumination for 60 min. The results indicating that the reaction is a photocatalytic driven process and the light, photocatalyst and scavenger play important role in the photocatalysis process.

To obtain the optimum reaction condition, controlled experiments have been carried out with different pH values. It can be found that the pH value of the reaction system could greatly influence the photocatalytic activity, as displays in Fig. 7. When the pH value in the solution decrease from 7 to 5, the reduction ratio of Cr(VI) increases rapidly with reduction ratio is 76.0%, 90.0% and 95.0%, respectively. By contrast, when the pH value is 3, the reduction of Cr(VI) almost 100% after 5 min irradiation. The reduction ratio of Cr(VI) over N-TiO_2 and ZnO are 61.0% and 7.6%, after visible light illumination for 60 min. The MIL-68(Fe) shows an efficient photocatalytic activity than that of N-doped TiO_2 and ZnO. The results reveal that the more acidic environment is benefit for the photocatalysis over MIL-68(Fe), which is similar to the previously

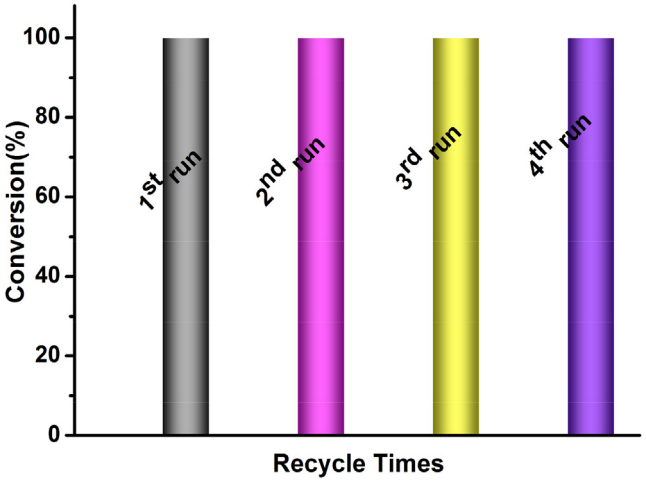

Fig. 8. Reusability of MIL-68(Fe) for photocatalytic reduction of Cr (VI). Reaction conditions: 10 mg photocatalyst, 40 mL of 20 ppm Cr (VI), 5 mg $(NH_4)_2C_2O_4$, pH = 3, λ > 420 nm.

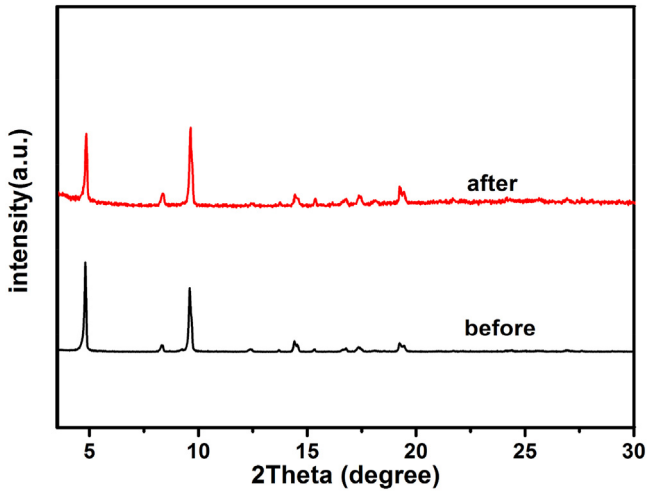

Fig. 9. XRD patterns of the MIL-68(Fe) before and after the photocatalytic reaction.

reported [37]. The zeta-potential (ξ) analysis results of MIL-68(Fe) in deionized water at different pH value (pH range of 3–7) show the surface of MIL-68(Fe) is dominated by positively charges. The surface charges of MIL-68(Fe) is pH 7 > pH 3 > pH 5 > pH 6 (9.91, 8.04, 7.54, and7.21 (Table S1)). Additionally, it's widely known that the Cr(VI) anionic will be reduced to Cr(III) ion (pH < 6) and $Cr(OH)_3$ (pH = 7), respectively. Generally, the positively charge surface of MIL-68(Fe) will be more beneficial to adsorb Cr(VI) anionic, thus leading to an enhanced reaction rate [38,39]. However, when the pH value is 7, the reduction production of $Cr(OH)_3$ will be precipitated on the surface of the photocatalyst. It results into shielding of the activity sites and decrease of photocatalytic activity [11]. In the comprehensive effects, the photocatalytic activity for reduction of Cr(VI) over MOFs follows the order: pH 3 > pH 5 > pH 6 > pH 7.

The stability is also of great importance to evaluate the photocatalyst. Fig. 8 illustrates the durability of photocatalytic activity of MIL-68(Fe) toward the reduction of Cr(VI) to Cr(III) under visible light illumination. Photocatalytic activity of MIL-68(Fe) does not obviously decrease after four cycles, suggesting that the MIL-68(Fe) possesses high photostability. Furthermore, The XRD (Fig. 9) and XPS results (Fig. 10) of the samples reveal that the crystal structure and surface chemical compositions of MIL-68(Fe) keep unchanged after the photocatalytic reaction. It is noteworthy that, the weak peak located at 577.59 eV can be observed in the narrow scan spectra of the Cr 2p, which is the typical binding energy peaks of Cr(III). The result further confirms that the Cr(VI) is reduced to Cr(III) in the photocatalytic reduction process (Fig. 10). The ICP analysis noticed that there is almost no Fe(III) ions leaching from the MIL-68(Fe) during the reaction (Table S2). These results suggest that the MIL-68(Fe) shows a good catalytic reusability and stability in this photocatalytic reaction.

As is known to all, industrial waste-water often contains significant amounts of heavy metal pollutants and hazardous organics (such as dyes). We have simulated a mixture solution contains Cr(VI) and hazardous dye (MG) with natural pH value to assess the photocatalytic performance of MIL-68(Fe) in treatment different categories of pollutants simultaneously. As shown in Fig. 11, for the single Cr(VI) systems, the reduction ratio is 13.0% after 4 h visible light irradiation. Obviously, it can be found the reduction ratio of Cr(VI) is increased dramatically after addition of MG. When the concentration of Cr(VI)/MG is 10 ppm/30 ppm, it shows the best removal rate of 94.5% and 80.3% (the ZnO only shows 4.6% and 61%, respectively). This could be attributed to the synergistic effect of photogenerated electrons and holes, the MG serves as the photogenerated holes scavenger and being oxidized, while Cr(VI) acts as photogenerated electrons acceptor and being reduced. The mineralization rate of C element is 40.7% in the mixed system of Cr(VI)/MG (Fig. S2), which is higher than that of ZnO (19.4%). The result of XRD after reaction reveals that crystal structure of MIL-68(Fe) keeps well (Fig. S3).

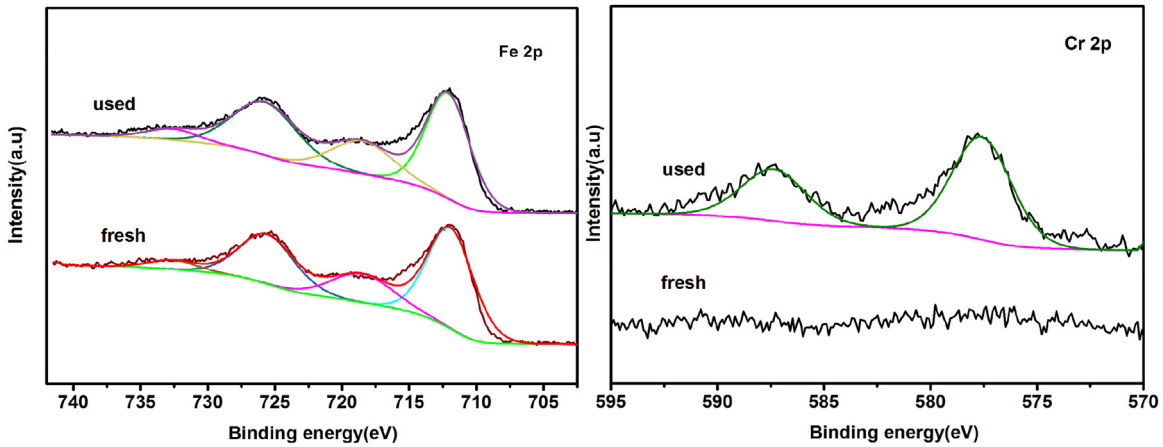

Fig. 10. XPS of Fe and Cr in the MIL-68(Fe) before and after the photocatalytic reaction of Cr (VI).

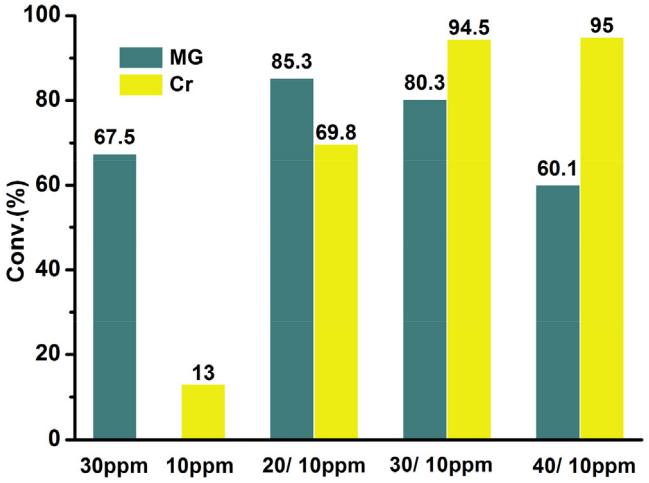

Fig. 11. Simultaneous photocatalytic reduction of Cr(VI) and degradation of organic dyes (MG) over MIL-68(Fe) under visible light irradiation. Reaction conditions: 10 mg photocatalyst, 40 mL mixture solution contain Cr(VI)/MG, λ > 420 nm.

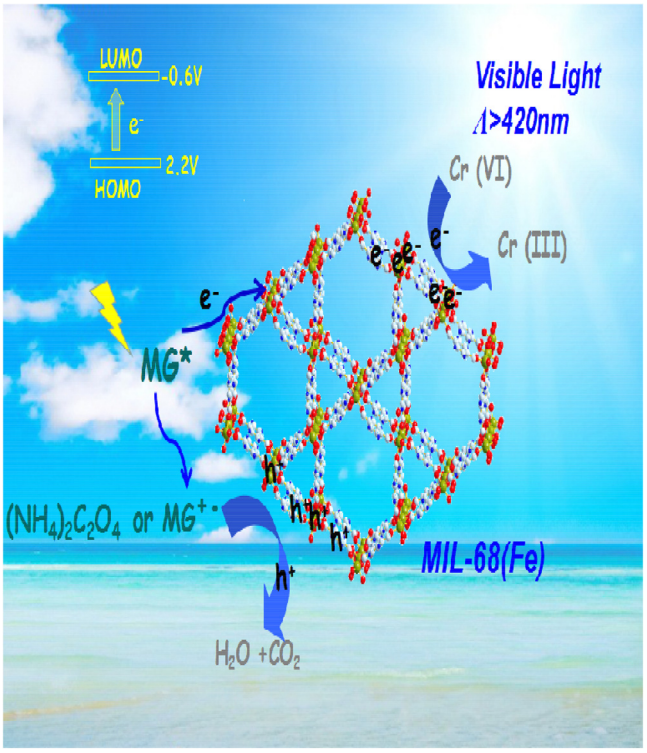

Fig. 12. Possible mechanism of photocatalytic for removal of aqueous contaminant over MIL-68(Fe).

On the basis of the above works, a probable reaction mechanism for removal of water contaminant over MIL-68(Fe) has been proposed and illustrated in Fig. 12. MIL-68(Fe) which consists of chains of corner-sharing $Fe(OH)_2O_4$ octahedral connected through a BDC (terephthalic acid) linker. Generally, the linker of MOFs can absorb visible light and excited electron transfer to the cluster [40,41]. As aforementioned (Fig. 4), the pure organic linker (H_2BDC) in MIL-68(Fe) does not absorb any visible light. Therefore, we can believe that the direct excitation of iron-oxo cluster is the main contributor to the photocatalytic performance of MIL-68(Fe), which has been observed in recently reported Fe(III)-based MOFs. Under visible light irradiation, the iron-oxo cluster in MIL-68(Fe) can absorb incident photons, then produces photoelectrons and photoholes [17,42]. On the other hand, the photoelectron can be produced after MG absorbs visible light and transfer to the iron-oxo cluster of MIL-68 [41]. Then the photogenerated charge carriers migrate to the surface of the MIL-68(Fe). The photogenerated electrons participate in the reduction reaction. While the photogenerated holes oxidize the organic pollution to CO_2 [43,44]. The synergetic effect of photogenerated electrons and holes results in a more efficient inhibition of photogenerated carriers combination. The possible reaction processes can be described as follows:

$$\text{MIL-68(Fe)}+h\nu \rightarrow \text{MIL-68(Fe)}(h^+ + e^-)$$

$$\text{MG} + h\nu \rightarrow \text{MG}^{+\cdot} + e^-$$

$$Cr_2O_7^{2-} + 14H^+ + 6e^- \rightarrow 2Cr^{3+} + 7H_2O$$

$$h^+ + \text{organic} \rightarrow CO_2 + H_2O$$

4. Conclusions

In summary, MIL-68(Fe) can behave as a pseodo-semiconductor with a suitable band gap (2.8 eV), HOMO (-0.6 V) and LUMO (2.2 V) energy. The as-prepared samples have been used as the high efficiency visible light-driven photocatalyst toward reduction of poisonous Cr(VI) aqueous solution. When pH = 3, after 5 min of visible light illumination (λ > 420 nm), almost 100% Cr(VI) can convert to Cr(III). While, the reduction rate of Cr(VI) reaches 76.0% after irradiation of 60 min with nature pH value. Further studies have demonstrated that the acidic conditions are more conducive to the reduction of Cr(VI), because positively charged MIL-68(Fe) is easily adsorb more negatively charged $Cr_2O_7^{2-}$ in acidic conditions. In addition, the addition of MG can enhance the photocatalytic reduction of Cr(VI) activity due to it can be oxidized by holes, which improves the separation of photogenerated charge carriers. The MIL-68(Fe) also exhibits excellent stability and dual-function photocatalytic performance in current photocatalytic reaction. It is hoped that our current work could enrich the application of Fe-MOFs photocatalysts in the field of simultaneously processed different water pollution.

Acknowledgement

This work was supported by the National Key Technology Research and Development Program of the Ministry of Science and Technology of China (2014BAC13B03).

Appendix A. Supplementary data

Supplementary data associated with this article can be found, in the online version, at http://dx.doi.org/10.1016/j.apcatb.2016.12.070.

References

[1] N.R. Bishnoi, M. Bajaj, N. Sharma, A. Gupta, Bioresour. Technol. 91 (2004) 305–307.
[2] J. Hu, G. Chen, I.M. Lo, Water Res. 39 (2005) 4528–4536.
[3] Y. Ku, I.-L. Jung, Water Res. 35 (2001) 135–142.
[4] P. Mohapatra, S.K. Samantaray, K. Parida, J. Photochem, Photobiol. A: Chem. 170 (2005) 189–194.
[5] J.J. Testa, M.A. Grela, M.I. Litter, Environ. Sci. Technol. 38 (2004) 1589–1594.
[6] X. Liu, L. Pan, Q. Zhao, T. Lv, G. Zhu, T. Chen, T. Lu, Z. Sun, C. Sun, Chem. Eng. J. 183 (2012) 238–243.
[7] J.L. Rowsell, O.M. Yaghi, Microporous Mesoporous Mat. 73 (2004) 3–14.
[8] H.-C. Zhou, J.R. Long, O.M. Yaghi, Chem. Rev. 112 (2012) 673–674.
[9] J.L. Rowsell, O.M. Yaghi, Angew. Chem. Int. Ed. 44 (2005) 4670–4679.
[10] J.-R. Li, R.J. Kuppler, H.-C. Zhou, Chem. Soc. Rev. 38 (2009) 1477–1504.

[11] R. Liang, L. Shen, F. Jing, W. Wu, N. Qin, R. Lin, L. Wu, Appl. Catal. B: Environ. 162 (2015) 245–251.
[12] L. Ma, C. Abney, W. Lin, Chem. Soc. Rev. 38 (2009) 1248–1256.
[13] P. Horcajada, C. Serre, M. Vallet-Regí, M. Sebban, F. Taulelle, G. Férey, Angew. Chem. 118 (2006) 6120–6124.
[14] P. Mahata, G. Madras, S. Natarajan, J. Phys. Chem. B 110 (2006) 13759–13768.
[15] M. Wen, Y. Cui, Y. Kuwahara, K. Mori, H. Yamashita, ACS Appl. Mater. Interfaces 8 (2016) 21278–21284.
[16] L. Shen, S. Liang, W. Wu, R. Liang, L. Wu, Dalton Trans. 42 (2013) 13649–13657.
[17] R. Liang, F. Jing, L. Shen, N. Qin, L. Wu, J. Hazar. Mater. 287 (2015) 364–372.
[18] R. Liang, R. Chen, F. Jing, N. Qin, L. Wu, Dalton Trans. 44 (2015) 18227–18236.
[19] R. Liang, S. Luo, F. Jing, L. Shen, N. Qin, L. Wu, Appl. Catal. B: Environ. 176 (2015) 240–248.
[20] A. Fateeva, P. Horcajada, T. Devic, C. Serre, J. Marrot, J.M. Grenèche, M. Morcrette, J.M. Tarascon, G. Maurin, G. Férey, Eur. J. Inorg. Chem. 2010 (2010) 3789–3794.
[21] J.-W. Zhang, H.-T. Zhang, Z.-Y. Du, X. Wang, S.-H. Yu, H.-L. Jiang, Chem. Commun. 50 (2014) 1092–1094.
[22] D. Wang, M. Wang, Z. Li, ACS Catal. 5 (2015) 6852–6857.
[23] Y.C. Zhang, J. Li, M. Zhang, D.D. Dionysiou, Environ. Sci. Technol 45 (2011) 9324–9331.
[24] C. Gong, D. Chen, X. Jiao, Q. Wang, J. Mater. Chem. 12 (2002) 1844–1847.
[25] P. Horcajada, C. Serre, G. Maurin, N.A. Ramsahye, F. Balas, M. Vallet-Regi, M. Sebban, F. Taulelle, G. Férey, J. Am. Chem. Soc. 130 (2008) 6774–6780.
[26] A. Banerjee, R. Gokhale, S. Bhatnagar, J. Jog, M. Bhardwaj, B. Lefez, B. Hannoyer, S. Ogale, J. Mater. Chem. 22 (2012) 19694–19699.
[27] S.K. Tam, J. Dusseault, S. Polizu, M. Ménard, J.-P. Hallé, L.H. Yahia, Biomaterials 26 (2005) 6950–6961.
[28] S.K. Das, M.K. Bhunia, M.M. Seikh, S. Dutta, A. Bhaumik, Dalton Trans. 40 (2011) 2932–2939.
[29] V. Chandra, J. Park, Y. Chun, J.W. Lee, I.-C. Hwang, K.S. Kim, ACS Nano 4 (2010) 3979–3986.
[30] M. Descostes, F. Mercier, N. Thromat, C. Beaucaire, M. Gautier-Soyer, Appl. Surf. Sci. 165 (2000) 288–302.
[31] T. Yamashita, P. Hayes, Appl. Surf. Sci. 254 (2008) 2441–2449.
[32] S. Bordiga, R. Buzzoni, F. Geobaldo, C. Lamberti, E. Giamello, A. Zecchina, G. Leofanti, G. Petrini, G. Tozzola, G. Vlaic, J. Catal. 158 (1996) 486–501.
[33] Y. Li, Z. Feng, H. Xin, F. Fan, J. Zhang, P.C. Magusin, E.J. Hensen, R.A. van Santen, Q. Yang, C. Li, J. Phys. Chem. B 110 (2006) 26114–26121.
[34] G. Vuong, M. Pham, T. Do, Dalton Trans. 42 (2013) 550–557.
[35] V. Spagnol, E. Sutter, C. Debiemme-Chouvy, H. Cachet, B. Baroux, Electrochim. Acta 54 (2009) 1228–1232.
[36] X. Wang, S. Pehkonen, A.K. Ray, Ind. Eng. Chem. Res. 43 (2004) 1665–1672.
[37] S. Congeevaram, S. Dhanarani, J. Park, M. Dexilin, K. Thamaraiselvi, J. Hazar. Mater. 146 (2007) 270–277.
[38] J. Gimenez, M. Aguado, S. Cervera-March, J. Mol. Catal. A: Chem. 105 (1996) 67–78.
[39] X. Hu, L. Lei, G. Chen, P.L. Yue, Water Res. 35 (2001) 2078–2080.
[40] Y. Fu, D. Sun, Y. Chen, R. Huang, Z. Ding, X. Fu, Z. Li, Angew. Chem. Int. Ed. 51 (2012) 3364–3367.
[41] M. Wen, K. Mori, T. Kamegawa, H. Yamashita, Chem. Commun. 50 (2014) 11645–11648.
[42] K.G. Laurier, F. Vermoortele, R. Ameloot, D.E. De Vos, J. Hofkens, M.B. Roeffaers, J. Am. Chem. Soc. 135 (2013) 14488–14491.
[43] N. Wang, L. Zhu, K. Deng, Y. She, Y. Yu, H. ppl. Tang, Catal. B: Environ. 95 (2010) 400–407.
[44] M. Asiltürk, F. Sayllkan, E. Arpac, J. Photochem. Photobiol. A 203 (2009) 64–71.